Introduction

Type 2 diabetes is a multifactorial disease caused by a complex interaction of environmental and genetic factors, with the latter consisting of multiple susceptibility genes, making it difficult to clarify their functions and interactions in conferring susceptibility to diabetes in humans. Inbred animal models of diabetes are therefore invaluable in dissecting such a complex interaction.

The Nagoya–Shibata–Yasuda (NSY) mouse was established as an inbred animal model with spontaneous development of type 2 diabetes by selective breeding for glucose intolerance from the closed colony of Jcl:ICR mice [1]. The phenotypes of the mouse resemble human type 2 diabetes in that the onset is age dependent, the animal is moderately obese and both impaired insulin response to glucose and insulin resistance contribute to the disease development [2–8]. Two quantitative trait loci (QTLs) on chromosome (Chr) 11 (*Nidd1n*) and Chr14 (*Nidd2n*), which affect glucose tolerance, have been identified in crosses of NSY mice with control C3H mice [7]. *Nidd1n* and *Nidd2n* have been suggested to affect glucose tolerance through impaired insulin secretion and insulin resistance, respectively [7]. The peaks of the linkage curve for *Nidd1n* and *Nidd2n* have been positioned in the region between *D11Mit236* (20.0 cM) and *D11Mit195* (47.0 cM) and in the region near *D14Mit59* (15.0 cM)/*D14Mit5* (22.5 cM) [7]. The regions showing significant linkage for *Nidd1n* and *Nidd2n* were broad, however, suggesting the possibility that multiple genes on the same chromosome contribute to the linkage of the regions, as was evidenced by the contribution of multiple susceptibility genes on the same chromosome to susceptibility to diabetes in the NOD mouse model of type 1 diabetes [9–11]. In fact, in addition to *Nidd1n* in the central part of Chr11, the existence of another locus near *D11Mit76* (2.0 cM), the most centromeric region on Chr11, distinct from the *Nidd1n* region, was suggested in our previous study [7].

The present study was performed to obtain direct evidence for susceptibility genes for type 2 diabetes on Chr11 and Chr14, and to clarify their function as well as interaction in conferring susceptibility to type 2 diabetes. To this end, we adopted a consomic approach [12], in which a whole chromosome of interest was introgressed onto the genetic background of the control strain. We first constructed two homozygous consomic strains, namely C3H-11^{NSY} and C3H-14^{NSY} mice, which carry an NSY-derived susceptible Chr11 or Chr14, respectively, on the control C3H background. Then, we established a double consomic strain, C3H-11^{NSY}14^{NSY}, containing both NSY-Chr11 and NSY-Chr14 in homozygous states on the C3H background. Various kinds of diabetes-related phenotypes of consomic strains have been monitored carefully and longitudinally. Finally, we performed sequence analysis of the glucokinase gene (*Gck*) on Chr11 (1.0 cM), as a functional candidate gene with peak linkage located in the centromeric region.

Methods

Animals

The NSY colony was maintained in the animal facilities of Osaka University Graduate School of Medicine. C3H/HeNcrj mice were purchased from Charles River Laboratories (Kanagawa, Japan). All mice had free access to tap water and a standard diet (CRF-1: Oriental Yeast, Tokyo, Japan) in an air-conditioned room (22–25°C) with a 12 h light–dark cycle (6:00–18:00 hours). Experimental designs were approved by the Osaka University Graduate School of Medicine Ethics Committee. Male mice were used for all experiments.

Construction of consomic strains (C3H-11^{NSY} and C3H-14^{NSY}) and double consomic strain (C3H-11^{NSY}14^{NSY})

C3H-11^{NSY} mice (Electronic supplementary material [ESM] Fig. 1) were produced by mating (NSY×C3H) F1 with C3H and selecting males that were heterozygous for the whole Chr11. These male mice were mated with C3H female mice, and their male progeny, heterozygous for the whole Chr11, were used for the next generation. In this process, we adopted a marker-assisted speed congenic method [13]. Namely, in every generation after the N3 generation, background genes were typed with polymorphic markers throughout the genome, and the best male mouse, which had the most substituted C3H genotype, was selected for breeding. This process was repeated until all the markers for background typing became homozygous for C3H genotypes (N6 or N7). Mice heterozygous for Chr11 were then intercrossed to obtain mice homozygous for Chr11. A total of four mice homozygous for NSY-derived Chr11 were obtained at the N6F1 (one out of 40 mice) and N7F1 (three out of 46 mice) generations. This line was maintained by brother–sister mating.

C3H-14^{NSY} mice (ESM Fig. 1) were constructed in the same way as for C3H-11^{NSY} mice. Five mice homozygous for NSY-derived Chr14 were obtained in the N8F1 generation (five out of 99 mice), and the line was maintained by brother–sister mating.

C3H-11^{NSY}14^{NSY} mice (ESM Fig. 1) were produced by mating (C3H-11^{NSY} × C3H-14^{NSY}) F1 with C3H-14^{NSY} and selecting mice that were homozygous for the NSY-derived allele at all loci on Chr14 and heterozygous for the NSY-derived allele at all loci on Chr11 (4/62 mice; 6.5%). These

mice were crossed with C3H-11^{NSY} to obtain mice that were homozygous for the NSY-derived allele at all loci on Chr11 and heterozygous for the NSY-derived allele at all loci on Chr14 (25/109 mice; 22.9%). Offspring that were homozygous for the NSY-derived allele at all loci on Chr14 as well as at all loci on Chr11 were selected (10/89 mice; 11.2%) and maintained by brother–sister mating.

Genotype analysis and localisation of markers

Genomic DNA was extracted from the tail. Information on microsatellite markers was obtained from the Mouse Genome Database (www.informatics.jax.org). The markers were amplified using PCR with primers with or without labels with 6FAM, NED or HEX. A total of 79 informative marker loci spanning the whole genome were analysed (ESM Table 1). In particular, we used 16 markers on Chr11 (average spanning less than 5 cM) and ten markers on Chr14 (average spanning less than 7 cM) to confirm no recombination, and to confirm none of the C3H-derived genome on Chr11 (in C3H-14^{NSY}) and Chr14 (in C3H-11^{NSY}). The non-labelled PCR products were electrophoresed on 9% polyacrylamide gels and visualised by ethidium bromide staining. The labelled PCR products were electrophoresed using an ABI 3100 sequencer (Applied Biosystems, Foster City, CA, USA) with GENESCAN 350 ROX (Applied Biosystems) as a size standard.

Phenotypic analysis

Assessment of glucose tolerance Glucose tolerance and body weight in NSY, C3H-11^{NSY}, C3H-14^{NSY}, C3H-11^{NSY}14^{NSY} and C3H mice were monitored longitudinally at 3, 6, 9 and 12 months of age. Glucose tolerance was assessed by intraperitoneal glucose tolerance test (ipGTT) (2 g glucose/kg body weight) in overnight-fasted mice, and blood glucose level was measured at 0, 30, 60, 90 and 120 min. The area under the glucose concentration curve (gAUC) was calculated according to the trapezoidal rule. Blood glucose level was measured directly by the glucose oxidase method using Glutest E (Kyoto Daiichi Kagaku, Kyoto, Japan).

Assessment of insulin secretion Insulin secretion in response to glucose was assessed by the insulinogenic index. IpGTT (2 g glucose/kg body weight) was performed as described above, and plasma insulin level was measured at 0, 15 and 30 min. Plasma insulin level was measured by ELISA (Morinaga, Yokohama, Japan). Incremental AUC ($\Sigma\Delta$gAUC) and incremental AUC ($\Sigma\Delta$iAUC) were calculated according to the trapezoidal rule from the glucose and insulin measurements at baseline (0 min), 15 and 30 min. Insulinogenic index was calculated as $\Sigma\Delta$iAUC÷$\Sigma\Delta$gAUC.

Assessment of insulin resistance HOMA-IR, as an indicator of insulin resistance, was calculated from the basal insulin and glucose concentrations (fasting glucose × fasting insulin).

Insulin tolerance test (ITT) was performed by injecting human insulin (0.25 U/kg) intraperitoneally in overnight-fasted mice at 3, 6, 9 and 12 months of age to evaluate insulin resistance longitudinally. Blood glucose level was measured at 0, 15, 30, 45 and 60 min.

Anatomical analysis Anatomical phenotypes were studied at 1 year of age. After anaesthesia by i.p. injection of pentobarbital sodium (Dainippon, Osaka, Japan), body weight and anal–nasal length were measured. BMI was calculated as body weight in grams divided by the square of anal–nasal length in centimetres Mice were killed under sevoflurane, and the epididymal, mesenteric, retroperitoneal fat pads and interscapular brown adipose tissue (BAT) were dissected and weighed.

Sequence analysis of Gck as candidate gene on chromosome 11 Genomic DNA was extracted from the livers of NSY and C3H mice. Fourteen pairs of primers (ESM Table 2) were designed so that the whole ten exons and exon–intron boundaries of *Gck* were covered. *Gck* produces two isoforms, beta cell-specific and liver-specific isoforms with alternative splicing, which are different in the promoter and first exon [14], so the primer pairs were designed separately for both. Genomic DNA was amplified by PCR with these primers, and the products were purified using a Wizard PCR Preps DNA Purification System (Promega, Madison, WI, USA). The sequencing reaction was performed using Big Dye Terminator (Applied Biosystems) according to the manufacturer's protocol, and the products were directly sequenced using an ABI 3100 sequencer (Applied Biosystems). To detect transcription binding sites, we used the TFSEARCH program (www.cbrc.jp/research/db/TFSEARCHJ.html) [15].

Statistical analysis

All results are expressed as mean ± SEM. Statistical analysis was performed by unpaired t test or one-way ANOVA. $p<0.05$ was regarded as significant.

Results

Longitudinal phenotypes of C3H-11^{NSY} mice

C3H-11^{NSY} mice had significantly higher blood glucose levels after fasting ($p<0.0001$) and at all time points after a glucose challenge ($p<0.0001$) than those in C3H mice at

12 months (Fig. 1a). No significant difference in body weight was observed between the two strains at any age, except at 3 months (Fig. 1b). In the longitudinal analysis of glucose tolerance, C3H-11^{NSY} mice showed significantly higher blood glucose levels than C3H mice at all ages studied ($p<0.0001$) (Fig. 1c). These results indicate that introduction of a single NSY-Chr11 can convert normoglycaemic C3H mice to hyperglycaemic mice without a change in body weight.

To better understand the mechanism of hyperglycaemia observed in C3H-11^{NSY} mice, we evaluated insulin secretion in response to glucose and insulin resistance longitudinally. The insulinogenic indices were significantly lower in C3H-11^{NSY} than in C3H mice at all ages (Fig. 1d). The glucose-lowering effect of insulin during ITT progressively worsened with age in C3H-11^{NSY} mice (Fig. 1e). The HOMA-IR value was significantly higher in C3H-11^{NSY} than in C3H mice at and after 6 months (Fig. 1f). These results suggest that both impaired insulin secretion in response to glucose and insulin resistance contribute to hyperglycaemia in C3H-11^{NSY} mice. Furthermore, the results suggest that impaired insulin secretion in response to glucose begins as early as at 3 months and remains constant thereafter, whereas insulin resistance begins at 6 months and gets worse with age in the C3H-11^{NSY} strain.

To further clarify the relationship of insulin resistance with body weight and abdominal fat accumulation in C3H-11^{NSY}, anatomical analysis was performed. As shown in Table 1, body weight and BMI in C3H-11^{NSY} mice were not significantly different from those in C3H mice. Fat-pad weight and the percentage of fat-pad weight/body weight were not significantly different either, suggesting that the age-dependent insulin resistance in C3H-11^{NSY} mice was independent of obesity and changes in fat accumulation.

Longitudinal phenotypes of C3H-14^{NSY} mice

C3H-14^{NSY} mice exhibited significantly higher blood glucose levels after fasting ($p<0.0001$) and at all time points after a glucose challenge ($p<0.0001$) than those in C3H mice at 12 months (Fig. 2a). Body weight was slightly heavier in C3H-14^{NSY} than in C3H mice at 3 and 6 months, but no significant difference was observed at and after 7 months (Fig. 2b). Longitudinal analysis of glucose tolerance during ipGTT showed significantly impaired glucose tolerance in C3H-14^{NSY} compared with that in C3H mice at all ages (Fig. 2c). No significant difference in the insulinogenic index was observed at any age between the two strains (Fig. 2d), suggesting that impaired insulin secretion in response to glucose did not contribute to hyperglycaemia in C3H-14^{NSY}

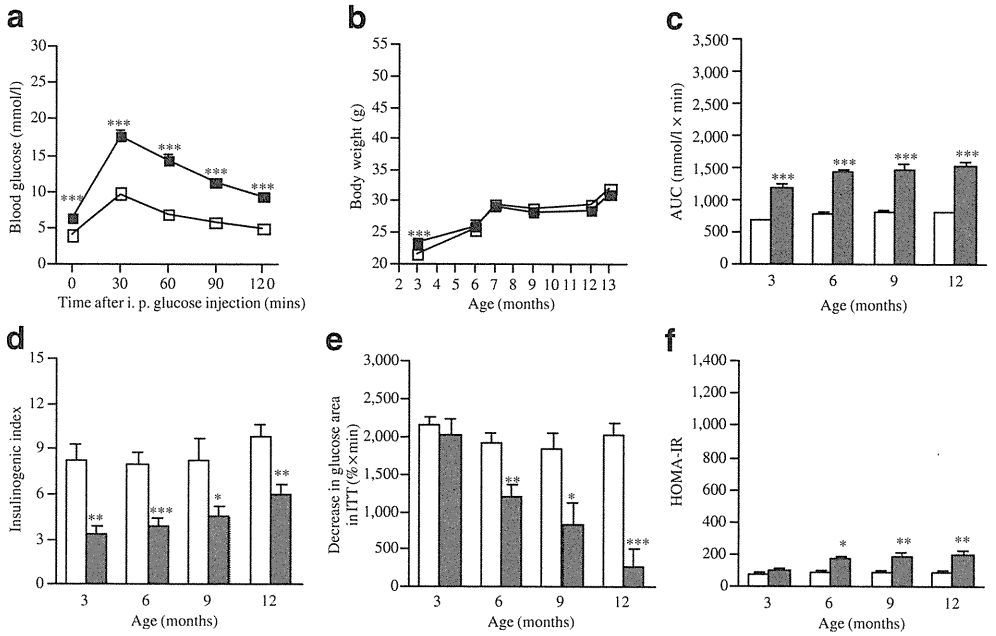

Fig. 1 Phenotypic analyses of C3H-11^{NSY}. **a** IpGTT at 12 months of age in C3H-11^{NSY} (n=28; black squares) and C3H mice (n=38; white squares). **b** Growth curve in C3H-11^{NSY} (n=17–56; black squares) and C3H mice (n=21–39; white squares). Body weight was measured after fasting (3, 6, 9 and 12 months) and under ad libitum feeding (7 and 13 months). **c–f** Longitudinal analyses of: (**c**) glucose tolerance (assessed by gAUC on ipGTT; n=28–56 C3H-11^{NSY} and n=33–39 C3H mice); (**d**) insulinogenic index (n=15–33 C3H-11^{NSY} and n=18–32 C3H mice); (**e**) insulin resistance (assessed by decrease in glucose area in insulin tolerance test; n=14–18 C3H-11^{NSY} and n=16–21 C3H mice); and (**f**) insulin resistance (assessed by HOMA-IR; n=15–33 C3H-11^{NSY} and n=18–32 C3H mice). C3H-11^{NSY} mice, grey bars; C3H mice, white bars. $^{*}p<0.05$, $^{**}p<0.01$, $^{***}p<0.0001$ compared with C3H

Table 1 Anatomical analysis in three consomic and parental strains at 12 months of age

Variable	NSY	C3H-11^{NSY}14^{NSY}	C3H-11^{NSY}	C3H-14^{NSY}	C3H
Number of mice analysed	11	18	26	19	19
Blood glucose (ad lib) (mmol/l)	9.4±0.6**	9.9±0.5**,††,‡‡	8.1±0.2*	6.9±0.2	6.8±0.2
Insulin (ad lib) (pmol/l)	928.6±122.8**,§§	448.1±60.0**,††	226.0±12.8	306.1±31.5	189.7±19.1
Body weight (g)	49.5±1.5**,§§	35.1±0.6**,††,‡‡	31.0±0.5	30.9±0.7	32.1±0.5
Anal–nasal length (cm)	11.1±0.1**,§§	10.5±0.1	10.4±0.0	10.2±0.1	10.3±0.0
BMI (g/cm^2)	0.403±0.008**,§§	0.319±0.004**,††,‡‡	0.288±0.004	0.296±0.005	0.300±0.003
Total fat (g)	3.269±0.151**,§§	1.736±0.107**,†	1.366±0.083	1.480±0.092	1.258±0.071
Epididymal fat (g)	1.356±0.076**,§§	0.946±0.068**,†	0.707±0.054	0.783±0.053	0.647±0.042
Retroperitoneal fat (g)	1.044±0.049**,§§	0.207±0.020	0.156±0.013	0.187±0.018	0.134±0.014
Mesenteric fat (g)	0.869±0.055**,§§	0.584±0.026*	0.502±0.021	0.510±0.029	0.476±0.022
Total fat/body weight (%)	6.63±0.30**,§§	4.90±0.24**	4.36±0.22	4.72±0.21*	3.85±0.19
BAT (mg)	201.3±18.2**,§§	139.5±7.1**,††,‡‡	77.6±4.7	84.8±4.8	93.1±6.3

Values are total number or mean ± SEM

The strains were compared by one-way ANOVA and post hoc test (Bonferroni): $^{*}p<0.05$, $^{**}p<0.01$ vs C3H; $^{\dagger}p<0.05$, $^{\dagger\dagger}p<0.01$ C3H-11^{NSY} 14^{NSY} vs C3H-11^{NSY}; $^{\ddagger\ddagger}p<0.01$ C3H-11^{NSY} 14^{NSY} vs C3H-14^{NSY}; $^{\S\S}p<0.01$ NSY vs C3H-11^{NSY} 14^{NSY}

Ad lib, ad libitum

mice. In contrast, the glucose-lowering effect of insulin during ITT was markedly and significantly impaired in C3H-14^{NSY} compared with that in C3H mice at and after 6 months (Fig. 2e). HOMA-IR was also significantly higher in C3H-14^{NSY} than in C3H mice at and after 6 months (Fig. 2f). These observations suggest that insulin resistance, but not impaired insulin secretion, contributed to glucose intolerance in the C3H-14^{NSY} strain.

To clarify the cause of insulin resistance in C3H-14^{NSY}, anatomical analysis was performed (Table 1). No significant

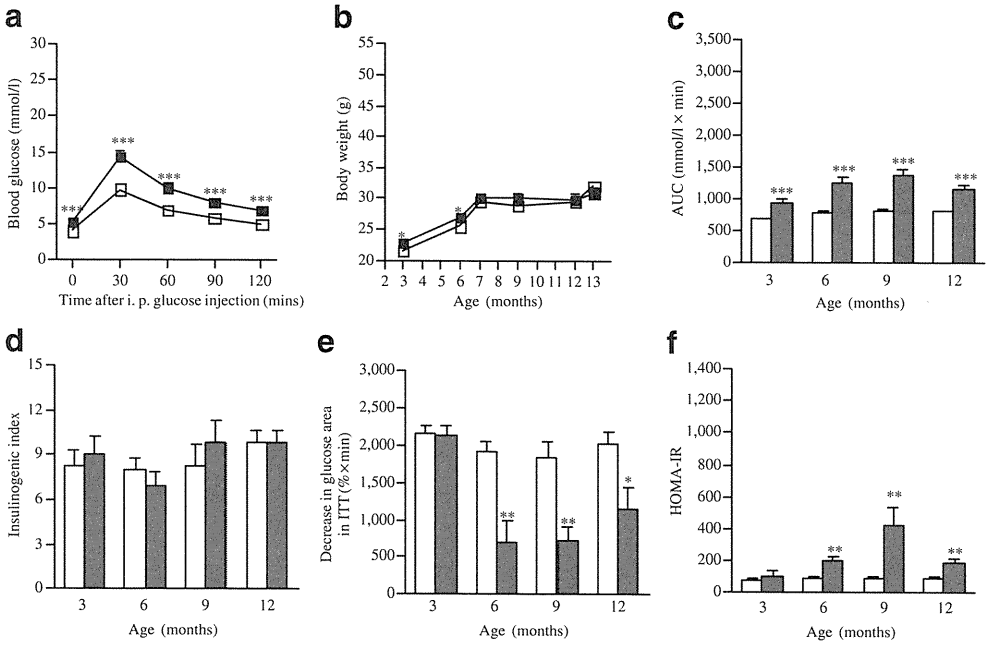

Fig. 2 Phenotypic analyses of C3H-14^{NSY}. **a** IpGTT at 12 months of age in C3H-14^{NSY} (n=32; black squares) and C3H mice (n=38; white squares). **b** Growth curve in C3H-14^{NSY} (n=15–36; black squares) and C3H mice (n=21–39; white squares). Body weight was measured after fasting (3, 6, 9 and 12 months) and under ad libitum feeding (7 and 13 months). **c–f** Longitudinal analyses of: (**c**) glucose tolerance (assessed by gAUC on ipGTT; n=26–36 C3H-14^{NSY} and n=33–39 C3H mice); (**d**) insulinogenic index (n=15–30 C3H-14^{NSY} and n=18–32 C3H mice); (**e**) insulin resistance (assessed by decrease in glucose area in insulin tolerance test; n=15–20 C3H-14^{NSY} and n=16–21 C3H mice); and (**f**) insulin resistance (assessed by HOMA-IR; n=15–30 C3H-14^{NSY} and n=18–32 C3H mice). C3H-14^{NSY} mice, grey bars; C3H mice, white bars. $^{*}p<0.05$, $^{**}p<0.01$, $^{***}p<0.0001$ compared with C3H

difference was observed in body weight, BMI and fat-pad weight between C3H-14^{NSY} and C3H mice. The percentage of fat-pad weight/body weight, however, was slightly but significantly elevated in C3H-14^{NSY} mice compared with C3H mice (Table 1), suggesting that an increase in the percentage of body fat may play a role in insulin resistance in C3H-14^{NSY} mice.

Longitudinal phenotypes of double consomic strain (C3H-11^{NSY}14^{NSY})

C3H-11^{NSY}14^{NSY} mice showed significantly higher blood glucose levels after fasting and after a glucose challenge than C3H mice ($p<0.0001$) (Fig. 3a) as well as single consomics, C3H-11^{NSY} ($p<0.05$) and C3H-14^{NSY} mice ($p<0.01$). Hyperglycaemia in C3H-11^{NSY}14^{NSY}, however, was not as severe as in NSY mice ($p<0.0001$ at 12 months) (Fig. 3a). Longitudinal analysis of glucose tolerance revealed that gAUC in C3H-11^{NSY}14^{NSY} was significantly higher than in C3H mice at all ages ($p<0.0001$), but not as high as in NSY mice (Fig. 3c). The insulinogenic index in C3H-11^{NSY}14^{NSY} mice was significantly lower than in C3H mice, and was similar to that in NSY mice at all ages (Fig. 3d). The glucose-lowering effect of insulin in C3H-11^{NSY}14^{NSY} mice was significantly impaired as compared with C3H mice at all ages (Fig. 3e). Insulin resistance in C3H-11^{NSY}14^{NSY} mice, however, was not as severe as in NSY mice (Fig. 3e, f). These results indicate that the major components of genetic susceptibility to hyperglycaemia in NSY were located on NSY-Chr11 and NSY-Chr14, but that other component(s) are also necessary for full reconstitution of the NSY phenotypes.

C3H-11^{NSY}14^{NSY} mice showed significantly higher body weight than C3H mice at all ages ($p<0.01$) (Fig. 3b), in contrast to no significant change in body weight in single consomics, C3H-11^{NSY} and C3H-14^{NSY}. These results provide direct evidence for a genetic interaction between NSY-Chr11 and NSY-Chr14, leading to obesity.

Diabetes-related phenotypes in single consomics, C3H-11^{NSY} and C3H-14^{NSY}, and double consomic, C3H-11^{NSY}14^{NSY}, in comparison with parental strains, NSY and C3H mice

As shown in Table 1, non-fasting blood glucose and insulin in C3H-11^{NSY}14^{NSY} and C3H-11^{NSY} mice were significantly higher than those in C3H mice, whereas no significant difference was observed between C3H-14^{NSY} and C3H mice. C3H-11^{NSY}14^{NSY} mice showed significantly higher body weight and BMI compared with C3H mice,

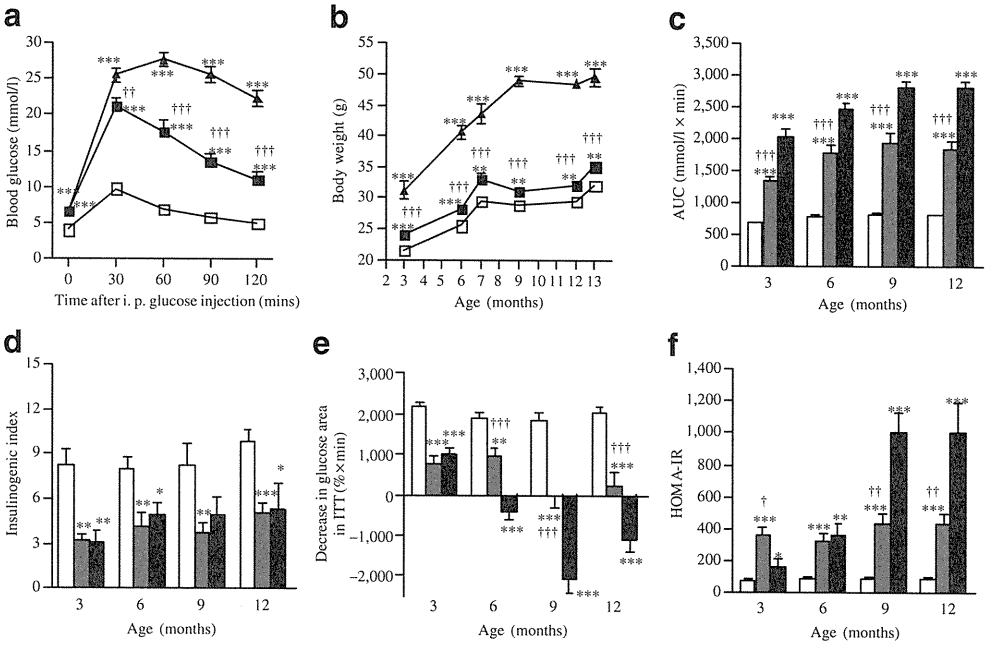

Fig. 3 Phenotypic analyses of C3H-11^{NSY}14^{NSY}. **a** IpGTT at 12 months of age in NSY (n=26; black triangles), C3H-11^{NSY}14^{NSY} (n=23; black squares) and C3H mice (n=38; white squares). **b** Growth curve in NSY (n=9–26; black triangles), C3H-11^{NSY}14^{NSY} (n=15–24; black squares) and C3H mice (n=21–39; white squares). Body weight was measured after fasting (3, 6, 9 and 12 months) and under ad libitum feeding (7 and 13 months). **c–f** Longitudinal analyses of: **c** glucose tolerance (assessed by gAUC on ipGTT; n=9–26 NSY, n=23–26 C3H-11^{NSY}14^{NSY} and n=33–39 C3H mice); **d** insulinogenic index (n=8–20 NSY, n=16–22 C3H-11^{NSY}14^{NSY} and n=18–32 C3H mice); **e** insulin resistance (assessed by decrease in glucose area in insulin tolerance test; n=9–19 NSY, n=20–23 C3H-11^{NSY}14^{NSY} and n=16–21 C3H mice); and **f** insulin resistance (assessed by HOMA-IR; n=8–20 NSY, n=16–22 C3H-11^{NSY}14^{NSY} and n=18–32 C3H mice). NSY mice, black bars; C3H-11^{NSY}14^{NSY} mice, grey bars; C3H mice, white bars. $^{*}p<0.05$, $^{**}p<0.01$, $^{***}p<0.0001$ compared with C3H

in contrast to no change in single consomic strains, C3H-11^{NSY} and C3H-14^{NSY} mice. Fat-pad weight and BAT in C3H-11^{NSY}14^{NSY} mice were significantly greater than in C3H mice, whereas C3H-11^{NSY} and C3H-14^{NSY} mice were not significantly different from C3H mice in these respects. Histologically, the heavier BAT showed deposition of fat, resembling white adipose tissue (data not shown), as was previously reported for mice with diet-induced obesity [16]. The percentage of fat-pad weight/body weight in C3H-11^{NSY}14^{NSY} and C3H-14^{NSY} mice was significantly higher than in C3H mice, whereas no significant difference was observed between C3H-11^{NSY} and C3H mice.

As shown in Table 2, C3H-11^{NSY}14^{NSY} showed hyperglycaemia, which appeared to be simply an additive, not synergistic, effect of NSY-Chr11 and NSY-Chr14. The insulinogenic index in C3H-11^{NSY}14^{NSY} mice was similar to that in C3H-11^{NSY} and parental NSY mice at all ages (Figs. 1d, 3d and Table 2), whereas that in C3H-14^{NSY} mice was similar to that in C3H mice at all ages (Fig. 2d and Table 2), suggesting that a major component(s) for impaired insulin secretion in response to glucose in NSY mice is located on Chr11. Insulin resistance in C3H-11^{NSY}14^{NSY} mice was greater than in C3H-11^{NSY} and C3H-14^{NSY} mice, but less than in NSY mice (Table 2). This suggests that major components for insulin resistance in NSY are located on both Chr11 and Chr14, but that these two chromosomes are not sufficient to fully reconstitute the phenotypes of the parental NSY mice.

DNA sequence of *Gck* as candidate gene on chromosome 11

The nucleotide sequences of *Gck*, spanning the 5′ upstream region, 5′ untranslated region (UTR), coding region and 3′ UTR, were determined in NSY (Accession number AB255658) and C3H (Accession number AB255659) mice. As shown in Fig. 4, a total of eight variants—seven single nucleotide polymorphisms (SNPs) and one insertion/deletion—were identified between NSY and C3H mice. The SNPs in introns were not located in exon–intron boundaries. Using the TFSEARCH program, the substitution in the 5′ upstream region was shown to be not located in the known *cis* element. When the variants identified between NSY and C3H mice were compared with reference sequences, six out of eight polymorphisms found in NSY mice were identical to those in C57BL/6 mice, and five out of eight polymorphisms were identical among NSY, 129SV and C57BL/6 mice, but they were different from those in C3H mice. The insertion polymorphism in C3H mice in the 3′ UTR was not found in the other three strains.

Discussion

This study clearly demonstrated that substitution of a single Chr11 or Chr14 from the diabetes-resistant C3H strain to the diabetes-susceptible NSY strain caused marked changes in diabetes-related phenotypes. The mechanisms of inducing hyperglycaemia, however, appeared to be different between C3H-11^{NSY} and C3H-14^{NSY} mice. NSY-Chr11 affects both insulin secretion and insulin sensitivity, whereas NSY-Chr14 affects insulin sensitivity but not insulin secretion. Interestingly, impaired insulin secretion in C3H-11^{NSY} was as severe as that in NSY mice, indicating that impaired insulin secretion in the NSY mouse could be accounted for mostly, if not totally, by Chr11. Despite the marked insulin resistance observed in C3H-11^{NSY} mice, no significant difference was observed in adiposity and obesity between

Table 2 Diabetes-related phenotypes in three consomic and parental strains at 12 months of age

Phenotypical component	NSY	C3H-11^{NSY}14^{NSY}	C3H-11^{NSY}	C3H-14^{NSY}	C3H
Glucose tolerance[a] (*n*)	2,800.9±91.5**,†† (26)	1,835.7±134.5**,‡,§§ (23)	1,535.2 ± 67.4** (28)	1,157.6±52.0** (32)	807.8±18.2 (38)
Insulin secretion[b] (*n*)	5.4±1.7** (13)	5.1±0.6**,§§ (22)	6.0±0.6* (19)	9.9±0.8 (30)	9.8±0.8 (32)
Insulin sensitivity (ITT)[c] (*n*)	−1,115.0±287.6**,†† (19)	231.9±309.2** (23)	264.2±243.2** (18)	1,146.9±299.8 (20)	2,034.0±144.0 (16)
Insulin sensitivity (HOMA-IR)[d] (*n*)	1,007.2±178.8**,†† (13)	436.3±63.9**,‡,§§ (22)	201.4±26.4 (19)	194.7±20.7 (30)	90.3±15.6 (32)

Values are total number or mean ± SEM

[a] Assessed by gAUC during ipGTT (mmol/l×min)

[b] Assessed by insulinogenic index (incremental AUC [ΣΔiAUC] [pmol/l]) divided by incremental gAUC ([ΣΔgAUC] [mmol/l]) during ipGTT

[c] Assessed by decrease in glucose area during ITT (%×min)

[d] Calculated from the basal insulin and glucose concentrations (fasting glucose [mmol/l]×fasting insulin [pmol/l])

The strains were compared by one-way ANOVA and post hoc test (Bonferroni): $^{*}p<0.05$, $^{**}p<0.01$ vs C3H; $^{††}p<0.01$ NSY vs C3H-11^{NSY} 14^{NSY}; $^{‡}p<0.05$ C3H-11^{NSY} 14^{NSY} vs C3H-11^{NSY}; $^{§§}p<0.01$ C3H-11^{NSY} 14^{NSY} vs C3H-14^{NSY}

n, number of mice analysed

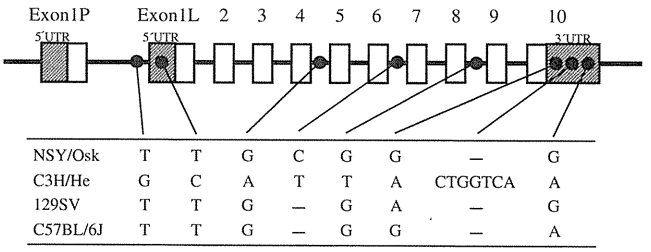

Fig. 4 Difference in *Gck* sequence between NSY and C3H. Exon 1P and exon 1L represent exon 1 of mRNA expressed in the pancreas and liver, respectively. Numbers represent exons. Black circles indicate different points in the sequence between NSY and C3H. Information on 129SV (Accession number L41631) and C57BL/6J strain were derived from an online database (www.ensembl.org/Mus_musculus). Dashes represent no base

C3H-11^{NSY} and C3H mice, suggesting that insulin resistance in C3H-11^{NSY} mice is independent of adiposity and obesity. In contrast, C3H-14^{NSY} mice showed a slight but significant increase in percentage fat-pad weight/body weight, suggesting that insulin resistance in C3H-14^{NSY} mice is at least in part associated with an increase in adiposity.

Type 2 diabetes develops when the pancreatic beta cell cannot compensate for insulin resistance [17]. The capacity of insulin secretion deteriorates with age, whereas insulin resistance increases with age, at least in common forms of type 2 diabetes under polygenic control. In this study, C3H-11^{NSY} mice showed that insulin secretion was impaired as early as at 3 months and continued to be impaired thereafter at any age. In contrast, insulin resistance worsened in an age-dependent manner. C3H-14^{NSY} mice did not show impaired insulin secretion at any age, but showed an age-related change in insulin resistance. These results demonstrate that each susceptibility gene(s) on Chr11 and Chr14 interacts with the ageing process in the development of insulin resistance, but not of insulin secretion.

In our previous mapping, F2 mice homozygous for NSY alleles at both *Nidd1n* and *Nidd2n* showed hyperglycaemia comparable with that in the parental NSY mouse [7]. These data, together with the marked phenotypic changes in each of the single consomic strains observed in the present study, suggest that type 2 diabetes in NSY may be oligogenic, with *Nidd1n* and *Nidd2n* accounting for most of the phenotypic changes in NSY. To ascertain whether or not *Nidd1n* and *Nidd2n* are sufficient to reconstitute most of the NSY phenotypes, a double consomic strain, C3H-11^{NSY}14^{NSY} with both *Nidd1n* and *Nidd2n*, was produced. Although the degree of hyperglycaemia in C3H-11^{NSY}14^{NSY} was greater than that observed in each single consomic, it was not as severe as that in NSY. These results suggest that additional genes on other chromosomes are necessary for the full expression of diabetes-related phenotypes of NSY mice. Moreover, in contrast to the absence of obvious obesity in each single consomic strain, C3H-11^{NSY}14^{NSY} mice showed significant obesity, demonstrating that genetic interaction between the two chromosomes plays a role in causing obesity. Thus, the present study clearly demonstrated that major components of genetic susceptibility to type 2 diabetes in NSY are located or clustered on Chr11 and Chr14, which can account for the majority of the phenotypic difference between NSY and C3H mice, but significant interaction between these two chromosomes as well as between these and other chromosomes is necessary for full reconstitution of the phenotypes.

The syntenic region on mouse Chr11 and Chr14 is human Chr17, 5q, 7p (for *Nidd1n*) and Chr3p, 10q, 8p, 13q (for *Nidd2n*). These regions are, therefore, considered to be candidate regions containing diabetogenic genes in humans. In fact, loci associated with type 2 diabetes have been mapped by whole-genome screening in humans [18–24]. More recently, many genome-wide or large-scale association studies revealed several candidate genes for type 2 diabetes and fasting glucose, such as *KCNJ11*, *KCNQ1*, *IGF2BP2*, *TCF7L2*, *MTNR1B*, *G6PC2*, and *GCKR* [25–29], although the orthologues of these genes are not located on mouse Chr11 and Chr14. In mice, linkages with type 2 diabetes were also reported on Chr11 [30–33] and Chr14 [34–37] in several independent crosses (ESM Table 3).

We previously reported sequence analyses of the genes for hepatocyte nuclear factor-1β, GLUT4 and nucleoredoxin [6, 7, 38–40]. In this study, we determined the nucleotide sequences of *Gck*, which is mapped in the centromeric region of Chr11. Although other positional candidate genes, such as genes for insulin-like growth factor binding protein (*Igfbp*) 1 and 3, are also located in the centromeric region of Chr11, *Gck*, which encodes glucokinase, a main glucose-phosphorylating enzyme acting as a glucose sensor of pancreatic beta cells, is a good functional candidate gene for QTL, which is located in the centromeric region of Chr11, because the QTL was linked to glucose/insulin ratio as well as hyperglycaemia [7]. Heterozygous mutations in the gene for human glucokinase, *GCK*, have been identified in patients with MODY [41, 42]. In the general population, a polymorphism in the beta cell-specific *GCK* promoter is associated with hyperglycaemia [43]. In mice, impaired insulin secretion and normal histology of pancreatic islets, as observed in C3H-11^{NSY} mice in the present study, were reported in mice with pancreatic beta cell-specific targeted disruption of *Gck* [44]. In a large scale mutagenesis project using *N*-ethyl-nitrosourea, it was reported that a number of mutations in *Gck* were identified in mice with the type 2 diabetes phenotype [45–47]. We found seven SNPs and one insertion/deletion polymorphism between NSY and C3H mice. The NSY allele is similar to that in C57BL/6 mice, but different from that in C3H mice. Interestingly, inbred control strains of mice have been reported to exhibit marked differences in glucose tolerance,

with C57BL/6 mice having the worst and C3H mice the best glucose tolerance [48]. It is therefore reasonable to speculate that the combination of variants with weaker effects in the non-coding SNPs in *Gck* results in susceptibility to common forms of type 2 diabetes, whereas functional mutations in exons cause a more severe form of diabetes, as in the case of MODY in humans [42]. Functional studies, including studies on insulin secretion in isolated islets, are necessary to clarify whether or not a variant of *Gck* is the cause of the insulin secretory defect in NSY, C3H-11^{NSY} and C3H-$11^{NSY}14^{NSY}$ mice.

In summary, the present study clearly provides direct evidence that Chr11 and Chr14 harbour diabetogenic genes in the NSY mouse. Introgression of each single chromosome onto control mice led to marked changes in phenotype. These two chromosomes interact to cause a more severe phenotype (hyperglycaemia) or a phenotype that was not observed in a single chromosome (obesity), suggesting a different mode of gene–gene interaction depending on the phenotype. The present study indicated the usefulness of the consomic strategy in proving the localisation as well as studying the functions and interactions of susceptibility genes for multifactorial diseases in general and diabetes-related phenotypes in particular, by dissecting disease-related phenotypes into each component. Marked changes in the phenotypes retained in the consomic strain will facilitate the fine mapping and the identification of the genes responsible and their interactions. The consomic strains established in the present study are also useful to study the interaction of genes on each chromosome with environmental factors in conferring susceptibility to diabetes. These studies are now under way.

Acknowledgements We thank M. Moritani for her skilful technical assistance and M. Shibata for his contribution to establishing the NSY colony and the discussion. This study was supported by a Grant-in-Aid for Scientific Research from the Ministry of Education, Science, Sports and Culture, Japan.

Duality of interest The authors declare that there is no duality of interest associated with this manuscript.

References

1. Shibata M, Yasuda B (1980) New experimental congenital diabetic mice (NSY mice). Tohoku J Exp Med 130:139–142
2. Hamada Y, Ikegami H, Ueda H et al (2001) Insulin secretion to glucose as well as nonglucose stimuli is impaired in spontaneously diabetic Nagoya–Shibata–Yasuda mice. Metabolism 50:1282–1285
3. Ikegami H, Fujisawa T, Ogihara T (2004) Mouse models of type 1 and type 2 diabetes derived from the same closed colony: genetic susceptibility shared between two types of diabetes. ILAR J 45: 268–277
4. Itoi-Babaya M, Ikegami H, Fujisawa T et al (2007) Fatty liver and obesity: phenotypically correlated but genetically distinct traits in a mouse model of type 2 diabetes. Diabetologia 50:1641–1648
5. Ueda H, Ikegami H, Kawaguchi Y et al (2000) Paternal–maternal effects on phenotypic characteristics in spontaneously diabetic Nagoya–Shibata–Yasuda mice. Metabolism 49:651–656
6. Ueda H, Ikegami H, Kawaguchi Y et al (2000) Age-dependent changes in phenotypes and candidate gene analysis in a polygenic animal model of Type II diabetes mellitus; NSY mouse. Diabetologia 43:932–938
7. Ueda H, Ikegami H, Kawaguchi Y et al (1999) Genetic analysis of late-onset type 2 diabetes in a mouse model of human complex trait. Diabetes 48:1168–1174
8. Ueda H, Ikegami H, Yamato E et al (1995) The NSY mouse: a new animal model of spontaneous NIDDM with moderate obesity. Diabetologia 38:503–508
9. Ghosh S, Palmer SM, Rodrigues NR et al (1993) Polygenic control of autoimmune diabetes in nonobese diabetic mice. Nat Genet 4:404–409
10. Todd JA, Aitman TJ, Cornall RJ et al (1991) Genetic analysis of autoimmune type 1 diabetes mellitus in mice. Nature 351:542–547
11. Wicker LS, Todd JA, Prins JB, Podolin PL, Renjilian RJ, Peterson LB (1994) Resistance alleles at two non-major histocompatibility complex-linked insulin-dependent diabetes loci on chromosome 3, Idd3 and Idd10, protect nonobese diabetic mice from diabetes. J Exp Med 180:1705–1713
12. Singer JB, Hill AE, Burrage LC et al (2004) Genetic dissection of complex traits with chromosome substitution strains of mice. Science 304:445–448
13. Markel P, Shu P, Ebeling C et al (1997) Theoretical and empirical issues for marker-assisted breeding of congenic mouse strains. Nat Genet 17:280–284
14. Magnuson MA, Shelton KD (1989) An alternate promoter in the glucokinase gene is active in the pancreatic beta cell. J Biol Chem 264:15936–15942
15. Heinemeyer T, Wingender E, Reuter I et al (1998) Databases on transcriptional regulation: TRANSFAC, TRRD and COMPEL. Nucleic Acids Res 26:362–367
16. Watanabe M, Houten SM, Mataki C et al (2006) Bile acids induce energy expenditure by promoting intracellular thyroid hormone activation. Nature 439:484–489
17. Kahn BB (1998) Type 2 diabetes: when insulin secretion fails to compensate for insulin resistance. Cell 92:593–596
18. Cai G, Cole SA, Freeland-Graves JH, MacCluer JW, Blangero J, Comuzzie AG (2004) Genome-wide scans reveal quantitative trait Loci on 8p and 13q related to insulin action and glucose metabolism: the San Antonio Family Heart Study. Diabetes 53: 1369–1374
19. Demenais F, Kanninen T, Lindgren CM et al (2003) A meta-analysis of four European genome screens (GIFT Consortium) shows evidence for a novel region on chromosome 17p11.2-q22 linked to type 2 diabetes. Hum Mol Genet 12:1865–1873
20. Duggirala R, Blangero J, Almasy L et al (1999) Linkage of type 2 diabetes mellitus and of age at onset to a genetic location on chromosome 10q in Mexican Americans. Am J Hum Genet 64: 1127–1140
21. Mitchell BD, Cole SA, Hsueh WC et al (2000) Linkage of serum insulin concentrations to chromosome 3p in Mexican Americans. Diabetes 49:513–516
22. Parker A, Meyer J, Lewitzky S et al (2001) A gene conferring susceptibility to type 2 diabetes in conjunction with obesity is located on chromosome 18p11. Diabetes 50:675–680
23. Pezzolesi MG, Nam M, Nagase T et al (2004) Examination of candidate chromosomal regions for type 2 diabetes reveals a susceptibility locus on human chromosome 8p23.1. Diabetes 53: 486–491
24. Reynisdottir I, Thorleifsson G, Benediktsson R et al (2003) Localization of a susceptibility gene for type 2 diabetes to chromosome 5q34–q35.2. Am J Hum Genet 73:323–335

25. Bouatia-Naji N, Bonnefond A, Cavalcanti-Proenca C et al (2009) A variant near MTNR1B is associated with increased fasting plasma glucose levels and type 2 diabetes risk. Nat Genet 41:89–94
26. Lyssenko V, Nagorny CL, Erdos MR et al (2009) Common variant in MTNR1B associated with increased risk of type 2 diabetes and impaired early insulin secretion. Nat Genet 41:82–88
27. Prokopenko I, Langenberg C, Florez JC et al (2009) Variants in MTNR1B influence fasting glucose levels. Nat Genet 41:77–81
28. Prokopenko I, McCarthy MI, Lindgren CM (2008) Type 2 diabetes: new genes, new understanding. Trends Genet 24:613–621
29. Reiling E, van't Riet E, Groenewoud MJ et al (2009) Combined effects of single-nucleotide polymorphisms in GCK, GCKR, G6PC2 and MTNR1B on fasting plasma glucose and type 2 diabetes risk. Diabetologia 52:1866–1870
30. Hirayama I, Yi Z, Izumi S et al (1999) Genetic analysis of obese diabetes in the TSOD mouse. Diabetes 48:1183–1191
31. Leiter EH, Reifsnyder PC, Flurkey K, Partke HJ, Junger E, Herberg L (1998) NIDDM genes in mice: deleterious synergism by both parental genomes contributes to diabetogenic thresholds. Diabetes 47:1287–1295
32. Takeshita S, Moritani M, Kunika K, Inoue H, Itakura M (2006) Diabetic modifier QTLs identified in F2 intercrosses between Akita and A/J mice. Mamm Genome 17:927–940
33. Toye AA, Lippiat JD, Proks P et al (2005) A genetic and physiological study of impaired glucose homeostasis control in C57BL/6J mice. Diabetologia 48:675–686
34. Almind K, Kahn CR (2004) Genetic determinants of energy expenditure and insulin resistance in diet-induced obesity in mice. Diabetes 53:3274–3285
35. Almind K, Kulkarni RN, Lannon SM, Kahn CR (2003) Identification of interactive loci linked to insulin and leptin in mice with genetic insulin resistance. Diabetes 52:1535–1543
36. Reifsnyder PC, Churchill G, Leiter EH (2000) Maternal environment and genotype interact to establish diabesity in mice. Genome Res 10:1568–1578
37. Suto J, Matsuura S, Imamura K, Yamanaka H, Sekikawa K (1998) Genetic analysis of non-insulin-dependent diabetes mellitus in KK and KK-Ay mice. Eur J Endocrinol 139:654–661
38. Babaya N, Ikegami H, Fujisawa T et al (2005) Susceptibility to streptozotocin-induced diabetes is mapped to mouse chromosome 11. Biochem Biophys Res Commun 328:158–164
39. Ueda H, Ikegami H, Kawaguchi Y et al (2001) Mapping and promoter sequencing of HNF-1beta gene in diabetes-prone and -resistant mice. Diabetes Res Clin Pract 53:67–71
40. Yamada K, Ikegami H, Kawaguchi Y et al (2001) Sequence analysis of candidate genes for common susceptibility to type 1 and type 2 diabetes in mice. Endocr J 48:241–247
41. Froguel P, Vaxillaire M, Sun F et al (1992) Close linkage of glucokinase locus on chromosome 7p to early-onset non-insulin-dependent diabetes mellitus. Nature 356:162–164
42. Gloyn AL (2003) Glucokinase (GCK) mutations in hyper- and hypoglycemia: maturity-onset diabetes of the young, permanent neonatal diabetes, and hyperinsulinemia of infancy. Hum Mutat 22:353–362
43. Rose CS, Ek J, Urhammer SA et al (2005) A −30G > A polymorphism of the beta-cell-specific glucokinase promoter associates with hyperglycemia in the general population of whites. Diabetes 54:3026–3031
44. Terauchi Y, Sakura H, Yasuda K et al (1995) Pancreatic beta-cell-specific targeted disruption of glucokinase gene. Diabetes mellitus due to defective insulin secretion to glucose. J Biol Chem 270:30253–30256
45. Aigner B, Rathkolb B, Herbach N, Hrabe de Angelis M, Wanke R, Wolf E (2008) Diabetes models by screen for hyperglycemia in phenotype-driven ENU mouse mutagenesis projects. Am J Physiol Endocrinol Metabol 294:E232–E240
46. Inoue M, Sakuraba Y, Motegi H et al (2004) A series of maturity onset diabetes of the young, type 2 (MODY2) mouse models generated by a large-scale ENU mutagenesis program. Hum Mol Genet 13:1147–1157
47. Toye AA, Moir L, Hugill A et al (2004) A new mouse model of type 2 diabetes, produced by N-ethyl-nitrosourea mutagenesis, is the result of a missense mutation in the glucokinase gene. Diabetes 53:1577–1583
48. Kaku K, Fiedorek FT Jr, Province M, Permutt MA (1988) Genetic analysis of glucose tolerance in inbred mouse strains. Evidence for polygenic control. Diabetes 37:707–713

Electronic supplementary material
ESM Fig. 1

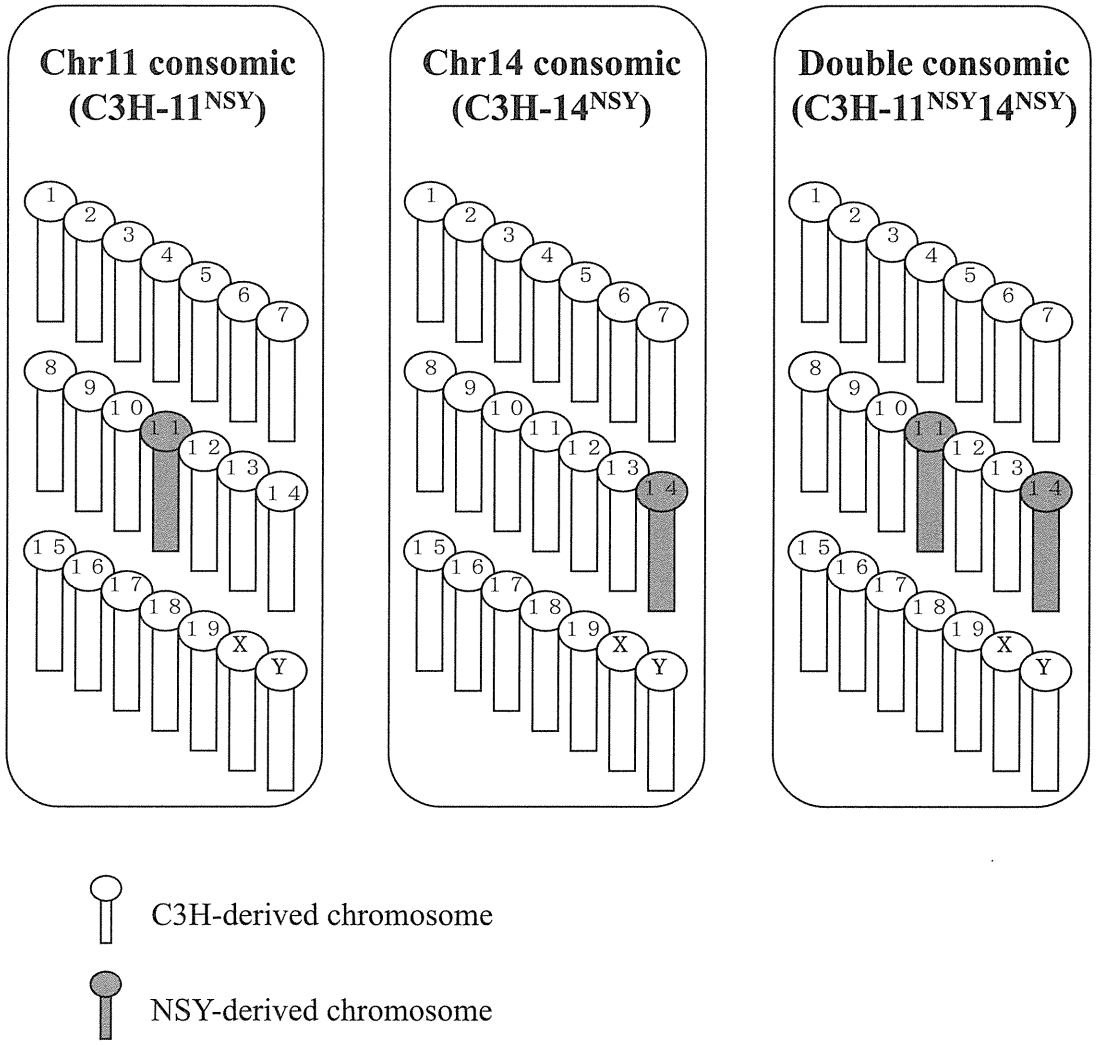

Electronic supplementary material

ESM Table 1 Polymorphic markers used in the study

Chromosome	Marker	(cM)	Chromosome	Marker	(cM)	Chromosome	Marker	(cM)	Chromosome	Marker	(cM)
Chr 1	*D1Mit173*	(23.6)	Chr 6	*D6Mit273*	(19.1)	Chr 11	*D11Mit74*	(0.0)	Chr 14	*D14Mit206*	(2.5)
	D1Mit19	(36.9)		*D6Mit178*	(38.5)		*D11Mit76*	(2.0)		*D14Mit207*	(5.5)
	D1Mit305	(55.1)		*D6Mit52*	(61.4)		*D11Mit229*	(14.0)		*D14Mit209*	(8.5)
	D1Mit14	(81.6)		*D6Mit14*	(71.2)		*D11Mit231*	(17.0)		*D14Mit186*	(10.0)
	D1Mit461	(102.0)					*D11Mit236*	(20.0)		*D14Mit59*	(15.0)
			Chr 7	*D7Mit20*	(5.5)		*D11Mit314*	(28.0)		*D14Mit5*	(22.5)
Chr 2	*D2Mit2*	(4.0)		*D7Mit62*	(42.6)		*D11Mit242*	(31.0)		*D14Mit235*	(28.2)
	D2Mit296	(18.0)		*D7Mit238*	(53.0)		*D11Mit156*	(34.0)		*D14Mit160*	(40.0)
	D2Mit37	(45.0)					*D11Mit320*	(43.0)		*D14Mit125*	(44.3)
	D2Mit304	(73.0)	Chr 8	*D8Mit171*	(8.0)		*D11Mit195*	(47.0)		*D14Mit266*	(60.0)
	D2Mit51	(95.5)		*D8Mit208*	(41.0)		*D11Mit286*	(52.0)			
				D8Mit167	(59.0)		*D11Mit70*	(54.0)	Chr 15	*D15Mit113*	(22.2)
Chr 3	*D3Mit117*	(2.4)					*D11Mit54*	(56.0)		*D15Mit123*	(30.6)
	D3Mit98	(39.7)	Chr 9	*D9Mit229*	(28.0)		*D11Mit145*	(57.5)		*D15Mit42*	(55.5)
	D3Mit257	(70.3)		*D9Mit269*	(43.0)		*D11Mit301*	(69.0)			
				D9Mit311	(65.0)		*D11Mit168*	(71.0)	Chr 16	*D16Mit88*	(9.7)
Chr 4	*D4Mit111*	(21.9)								*D16Mit4*	(27.3)
	D4Mit219	(49.6)	Chr 10	*D10Mit194*	(29.0)	Chr 12	*D12Mit270*	(13.0)		*D16Mit158*	(54.5)
	D4Mit48	(69.8)		*D10Mit230*	(49.0)		*D12Mit255*	(38.0)			
				D10Mit164	(67.5)		*D12Mit20*	(58.0)	Chr 17	*D17Mit36*	(24.5)
Chr 5	*D5Mit148*	(18.0)								*D17Mit206*	(44.5)
	D5Mit41	(56.0)				Chr 13	*D13Mit13*	(35.0)			
	D5Mit262	(72.0)					*D13Mit74*	(59.0)	Chr 18	*D18Mit35*	(24.0)
							D13Mit78	(75.0)		*D18Mit7*	(50.0)
									Chr 19	*D19Mit80*	(22.0)
										D19Mit34	(53.0)

The map positions of SSLPs (in parentheses) were obtained from the Mouse Genome Database (www.informatics.jax.org)

Electronic supplementary material

ESM Table 2 Sequences of polymerase chain reaction primers used for amplification of *Gck*

Region	Forward primer (5'–3')	Reverse primer (5'–3')
β cell-specific exon 1A	GGG CTC TGC TCC TTA GTG TG	TTG AAG CCA CAG CTT CCT CT
β cell-specific exon 1B	ACA TGG CTC CTC CTG AAG AC	AGA GAT CTT TCT GCC CGA CA
Liver-specific exon 1	CTG ATC CCA CGT GGT TCT TT	GTG GAC TCC TCA AGA GCT GG
Exon 2	CAG AGG ACC AAA AGA GAC C	TGA CCC AGA GAC AAA AAG G
Exon 3	CAC CTT TGA CCC TTC CAC A	TTG CTG CTG ACC TTT CTT C
Exon 4	TGC CTC CCA TTG TCC CTA AG	CCA CCC ATT CAT CTC CTC TC
Exon 5 and exon 6	TGT GAA ACA AGG TGT TGG GA	TGA GTG CTA TGA GCC TGT GC
Exon 7	AAA TGT GCC TCA TCC CGT AG	CAA CTT GCT TCT CCC CAG AG
Exon 8	TAA CCA GAA TAG GGC GCT TG	CCC ACT TCA TCC CTC TGT GT
Exon 9	GAC TTC CCT CCC TAA TAC C	CAC CCC TCA GCC CAG ACT
Exon 10A	GTG GCA AAG GTG GGA TCT AA	TGT CTC ACT GGC TGA CTT GG
Exon 10B	GAC TCC ACA CCC CAC AAA TG	CGC AGC CTC TTC AGC CAC AG
Exon 10C	AGG TAG CTT CAG CAG CTT GG	AAA CCT GAC AGG GAT GAT GG
Exon 10D	AAG CAA GCC ACC CAC AGC AT	GCC TCC ACA TTC CTA TTC CT

Electronic supplementary material

ESM Table 3 Correspondence of diabetogenic loci on chromosomes 11 and 14 reported here with loci linked with diabetes and related phenotypes reported in other mapping studies

Chromosome	Linked marker	Position (cM)	Cross	Phenotype	Reference
11	*D11Mit1*	2.4	C57BL/6 × C3H	Fasting glucose level	[1]
11	*D11Mit242*	31.0	NSY × C3H	Blood glucose level	[2][a]
11	*D11Mit41*	49.0	NZO × NON	Serum insulin level	[3]
11	*D11Mit128*	68.0	TSOD × BALB/c	Blood glucose level	[4]
11	*D11Mit254*	75.4	Akita × A/J	Blood glucose level	[5]
14	*D14Mit55*	10.5	C57BL/6 × 129S6	Blood glucose level	[6]
14	*D14Mit52*	11.5	C57BL/6 × 129S6	Insulin resistance	[7]
14	*D14Mit212*	13.5	NZO × NON	Adiposity	[8]
14	*D14Mit5*	22.5	NSY × C3H	Blood glucose level	[2][a]
14	*D14Mit192*	40.0	C57BL/6 × 129S6	Body weight	[7]
14	*D14Mit165*	52.0	KK × C57BL/6	Fasting glucose level	[9]

The map positions were obtained from the Mouse Genome Database (www.informatics.jax.org)

[a]Our previous study. The representative marker was picked up because the position of the QTL peaks changed according to the age and the peaks were broad

References

1. Toye AA, Lippiat JD, Proks P et al (2005) A genetic and physiological study of impaired glucose homeostasis control in C57BL/6J mice. Diabetologia 48:675–686
2. Ueda H, Ikegami H, Kawaguchi Y et al (1999) Genetic analysis of late-onset type 2 diabetes in a mouse model of human complex trait. Diabetes 48:1168–1174
3. Leiter EH, Reifsnyder PC, Flurkey K, Partke HJ, Junger E, Herberg L (1998) NIDDM genes in mice: deleterious synergism by both parental genomes contributes to diabetogenic thresholds. Diabetes 47:1287–1295
4. Hirayama I, Yi Z, Izumi S et al (1999) Genetic analysis of obese diabetes in the TSOD mouse. Diabetes 48:1183–1191
5. Takeshita S, Moritani M, Kunika K, Inoue H, Itakura M (2006) Diabetic modifier QTLs identified in F2 intercrosses between Akita and A/J mice. Mamm Genome 17:927–940
6. Almind K, Kulkarni RN, Lannon SM, Kahn CR (2003) Identification of interactive loci linked to insulin and leptin in mice with genetic insulin resistance. Diabetes 52:1535–1543
7. Almind K, Kahn CR (2004) Genetic determinants of energy expenditure and insulin resistance in diet-induced obesity in mice. Diabetes 53:3274–3285
8. Reifsnyder PC, Churchill G, Leiter EH (2000) Maternal environment and genotype interact to establish diabesity in mice. Genome Res 10:1568–1578
9. Suto J, Matsuura S, Imamura K, Yamanaka H, Sekikawa K (1998) Genetic analysis of non-insulin-dependent diabetes mellitus in KK and KK-Ay mice. Eur J Endocrinol 139:654–661

第5章　各種データ解析

第2節　SNP解析

1. はじめに

SNP(single nucleotide polymorphism)タイピング技術の進展に伴って，ヒトのさまざまな多因子疾患に関わる遺伝子を探索する戦略としてゲノムワイド関連研究(genome-wide association study；GWAS)が近年大きな注目を浴びている。ヒト多因子疾患の疾患感受性遺伝子を探索する統計遺伝学的手法には，大別して連鎖分析(linkage analysis)と関連分析(association analysis)がある。連鎖分析は患者家族を対象として，文字通り疾患遺伝子と多型マーカーの連鎖を検出する手法であり，ゲノム全域に分布する1万から数万種のSNPを用いれば十分である。一方，関連分析の代表であるケース・コントロール関連分析法は非血縁の患者群と健常対照群を対象として，疾患遺伝子と多型マーカーの連鎖不平衡(linkage disequilibrium)を検出する手法であり，これをゲノム全域にわたって適用するGWASでは数十万種以上のSNPあるいは数万種以上のマイクロサテライトマーカーを解析することが必要となる[1]。なお，このGWASは日本の研究者によって先駆的に行われ，これまでにいくつかのヒト多因子疾患の感受性遺伝子を特定することに成功している[2~5]。また，2003年からオーダーメイド医療実現基盤を構築することを目標とした「オーダーメイド医療実現化プロジェクト」が開始され，30万人の日本人を対象とした遺伝情報解析が行われている[6]。2008年には，日本における2大プロジェクトである「オーダーメイド医療実現化プロジェクト」と「ミレニアムゲノムプロジェクト」からそれぞれ独立に2型糖尿病に関連する遺伝子である*KCNQ1*を発見したという報告がなされた[7][8]。また，筆者らの研究室においても，*CPT1B*遺伝子と*CHKB*遺伝子の間に存在するSNPが睡眠障害の1つであるナルコレプシーと関連していることを発見し，2008年に報告をした[9]。

SNPタイピング法としてもっともよく知られている方法は，個々の多型部位を含む領域をPCR(polymerase chain reaction)で特異的に増幅した後にアリルを識別する方法である[10~14]。これらの方法では，1,000種程度のSNPを対象としたタイピングであれば，PCRプライマーをはじめとする各種試薬にかかるコストを考えても実用可能であるといえるが，数千から数万種を超える数のSNPをタイピングすることは困難となる。一方，近年になって多型部位特異的なPCRを行わずに大規模なSNPタイピングを行う方法が実用化された[15][16]。その1つであるAffymetrix社によって確立された方法では，まず制限酵素反応でゲノムDNAの断片化を行い，続いてそれら断片の両端にアダプター配列を付加し，まとめて増幅した後にマイクロアレイを用いたアリル特異的なハイブリダイゼーションを行う[15]。現在では，この手法を用いて90万種を超えるSNPを同時にタイピングするキットが市販されている(Affymetrix® Genome-Wide Human SNP Array 6.0，以下SNP Array 6.0)。筆者らの教室に設置したヒトSNPタイピングセンターではSNP Array 6.0によるSNPタイピングを効率的に行うためのシステムを構築し，いくつかの多因子疾患についてゲノムワイド関連分析を実施している。

SNP Array 6.0に搭載されたSNPは，公共のSNPデータベースおよびPerlegen社に登録された約220万種のSNPから遺伝学的情報量が最大化されるように，また連鎖不平衡やHapMapプロジェクトからの情報も考慮して選択された約44万種のSNPに，Tag SNP，X染色体およびY染色体に存在するSNP，ミトコンドリアSNPなどを加えた全909,622種のSNPである。全90万種のSNPについ

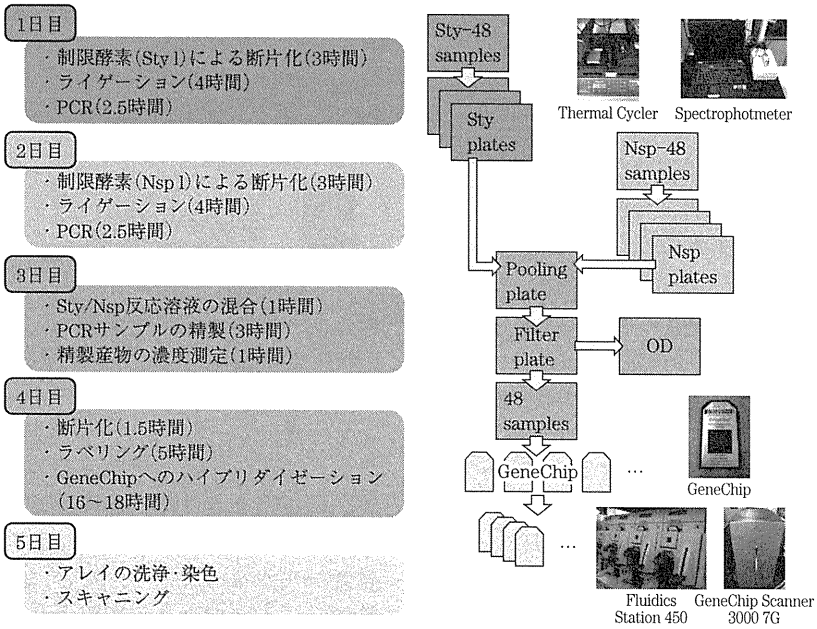

図1　SNP Array 6.0 による SNP タイピングの流れ

制限酵素(Sty I, Nsp I)による断片化反応からスキャニングまで全5日の工程で SNP タイピングが行われる。1検体につき 500 ng のゲノム DNA を用いて全 909,622 種の SNP をタイピングすることができる。

て，HapMap の3集団(Caucasian, African, Asian)におけるマイナーアリル頻度(minor allele frequency；MAF)の平均は，それぞれ 19.6%，20.6%，18.2% である。しかしながら，HapMap プロジェクトでは 45 検体の日本人しか解析していないため，MAF の低い SNP については正確な頻度推定ができない[17]。そこで，筆者らは SNP Array 6.0 を用いて日本人健常者 200 検体を解析し，日本人を対象とした GWAS において統計解析に用いることのできる SNP 数を算出することを試みた[18]。また，SNP Array 6.0 は遺伝子型を決定するために Birdseed アルゴリズムを用いるが，Birdseed アルゴリズムを用いた遺伝子型決定の精度を上げることが，ゲノムワイド関連分析における偽陽性関連を効果的に排除することにつながる。そこで，日本人健常者 200 検体のタイピング結果を用いて，Birdseed アルゴリズムによる正確な遺伝子型決定方法を検討した[18]。

2. SNP Array 6.0 の技術原理

SNP Array 6.0 による SNP タイピングは，ゲノムの複雑さを低減しマイクロアレイへのハイブリダイゼーション効率を上げるための酵素反応ステップと，洗浄・染色装置(Fluidics Station 450)およびマイクロアレイ用スキャナ(GeneChip Scanner 3000 7G)を用いた検出ステップで構成される(**図1**)。SNP タイピングは1検体につき合計 500 ng のゲノム DNA を使用し，2種類の制限酵素(Sty I, Nsp I)を用いて実現される。制限酵素によるゲノム DNA の断片化を行った後，断片化されたゲノム DNA の両末端にアダプター配列をライゲーション反応により付加する。アダプター配列は，続く PCR で使用されるプライマーと相同な配列をもち，また制限酵素認識配列を突出端として持つ二本鎖 DNA である。2種類の制限酵素(Sty I, Nsp I)のそれぞれに対して用意されるアダプター配列は，制限酵素認識配列を除いて共通の配列をもっているので共通のプライマを使用して PCR を行うことができる。PCR では，目的の長さをもった DNA 断片(250～1100 bp)だけが選択的に増幅される。ここまでの酵素反応により，もともと 30 億塩基対のゲノム DNA が5億塩基対程度の PCR 混合産物となる。マイクロアレイへの効率的なハイブリダイゼーションには，ゲノムの複雑さを低減することが大きな役割を果たす

と考えられている[19]。続いて，Sty I およびNsp I それぞれのPCR産物を混合した後，混合産物を精製し，DNase I制限酵素による断片化を行う。ここで断片化されたPCR産物は平均長で180 bp以下となる。マイクロアレイへの効率的なハイブリダイゼーションには，ゲノムの複雑さを低減することに加えてPCR産物の断片化が重要になる。最後にterminal deoxynucleotidyl transferase酵素反応により，断片化されたPCR産物の末端にビオチンを導入する。

続いて，専用のマイクロアレイ(GeneChipアレイ)を用いてハイブリダイゼーションを行う。マイクロアレイに固定されるプローブは25塩基長のオリゴDNAで，SNP部位を含む塩基配列をもっている。2種類のアリルを正確に識別するために，SNP部位を25塩基長のプローブの中心に置いたプローブを基本として，SNP部位を中心から4塩基上流(+4)にずらしたプローブから4塩基下流(−4)にずらしたプローブまで7種類のプローブ(−4，−2，−1，0，+1，+3，+4)を用意し，その中から最適な1種類のプローブを選択する。また，同一のプローブをマイクロアレイ上に3スポット用意することで，SNPタイピングデータの欠損を防ぐ工夫がなされている。

マイクロアレイへのハイブリダイゼーションが終了した後，洗浄・染色装置を用いてマイクロアレイの洗浄および蛍光染色を行う。蛍光染色は，蛍光分子で標識されたストレプトアビジンが，上述のビオチン導入されたPCR断片に結合することにより行われる。また，洗浄・染色装置内ではビオチン修飾された抗ストレプトアビジン抗体を用いてシグナルの増強が行われる。最後に蛍光染色されたマイクロアレイを専用のスキャナで画像データとして読み取り，続いて専用のソフトウェアを用いて各SNPの遺伝子型を決定する。

複数の施設で行われたSNP Array 6.0によるSNP解析の結果から，Overall call rate(全909,622 SNPsのうち遺伝子型が決定されたSNPの割合)は平均99%以上となり，また，HapMapデータベースに登録されたSNPとの遺伝子型一致率は99.7%を超えることがAffymetrix社から報告されている。また，タイピング結果が悪いことが明らかとなっている3,022種のSNPをクオリティーコントロール(QC)として用いて，QC call rate(3,022種のSNPのうち遺伝子型が決定されたSNPの割合)が86%を下回る検体を除外したうえで全SNPの遺伝子型は決定される。

3. システム構築

3.1 ハードウェアの整備

SNP Array 6.0によるSNPタイピングを効率的に行うために，環境，装置を整備し，作業マニュアルを作成した。まず，ゲノムDNAへのPCR産物のコンタミネーションを防ぐために，試料調製室とSNP解析室を設けた。試料調製室にはゲノムDNAを保管し，PCRまでの酵素反応を行うのに必要な装置(サーマルサイクラーなど)を用意した。制限酵素(Sty I，Nsp I)による断片化からPCRの反応溶液の調製までを試料調製室で行い，PCR以降の酵素反応はSNP解析室で行った。また，5台の洗浄・染色装置を用意し，1回のランで計20枚のマイクロアレイを洗浄・染色することができるようにした。すべてのマイクロアレイはバーコードで管理され，洗浄・染色が終了したマイクロアレイはオートローダ付きのマイクロアレイ用スキャナに装填され画像データが読み込まれる。オートローダ付きのマイクロアレイ用スキャナは計64枚のマイクロアレイを装填することができ，バーコードを参照しながらすべてのマイクロアレイの画像データを自動的に読み込むことができる。

SNPタイピング作業のルーチン化にあたって，制限酵素(Sty I，Nsp I)による断片化からラベリングまでの酵素反応ステップで使用するすべてのマイクロタイタープレートをバーコードで管理する。また，48検体を1バッチとして酵素反応を行うこととし，マイクロタイタープレートのウェル位置をサンプルと対応させることでサンプルのID化を行った。マイクロタイタープレート上のレイアウトを変えずに酵素反応を進めることで，ウェル位置をサンプルIDとして解析結果を得ることができる。また，酵素反応の各工程を管理するためにチェックシートを作成し，反応工程の進行を随時チェックシートで確認しながら進める。PCRおよびDNase I制限酵素による断片化の後にはアガロースゲル電気泳動を行い，PCR産物の平均長が250〜1,100 bpとな

っていること，また断片化産物の平均長が180 bp以下となっていることを確認する。加えて，精製後のPCR産物の濃度が500～600 ng/μlとなっていることを確認する。

3.2　ソフトウェアの開発

SNP Array 6.0によるSNPタイピングではメーカーが提供する2種類のソフトウェアを使用する(GeneChip Operating System(GCOS)，Genotyping Console 3.0(GTC 3.0))。GCOSは洗浄・染色装置およびマイクロアレイ用スキャナを操作する際に使用し，またGTC 3.0はマイクロアレイの蛍光強度データ(CELファイル)から遺伝子型を判定する際に使用する。決定された全909,622種のSNPの遺伝子型は，検体ごとにテキストファイルとしてエクスポートすることができる。

筆者らが開発したゲノムワイド関連分析用ソフトウェア(Gene Chip Analysis ver 2.0.12)は，エクスポートしたテキストファイルを直接入力ファイルとして用いることができる。また，ケース・コントロール関連分析をするにあたって各検体から全SNPの遺伝子型データを抽出し，さらにすべての検体をケース群およびコントロール群に分けて新たなテキストファイルとして作成する機能をソフトウェアに加えた。全909,622種のSNPについて，アリル頻度，ジェノタイプ頻度，優性・劣性モデルでのケース・コントロール関連分析を行うことができ，関連分析の結果は専用のソフトウェア(Gene Chip Viewer ver 2.1.1)を用いて視覚的に表示することができる。

4.　日本人健常者200検体のSNPタイピングデータの解析結果

SNP Array 6.0によるSNPタイピングでは，Sty IおよびNsp Iによる断片化反応に用いるゲノムDNA量がそれぞれ250 ngとなるように調整することがSNPタイピングの精度に大きな影響を与えることがこれまでの実験結果から明らかとなっている[18]。日本人健常者200検体のうち195検体のゲノムDNA濃度は規定濃度である50 ng/μlを満たしており，平均54.8 ng/μlであったが，5検体は規定濃度を下回り平均41.1 ng/μlであった。そこで，規定濃度を下回った5検体は制限酵素断片化反応に6 μlを持ち込み，ゲノムDNAの総量が約250 ngとなるように調整してタイピングを行うこととした。日本人健常者200検体のSNPタイピングを行った結果，QC call rateは平均97.37%となり，また，

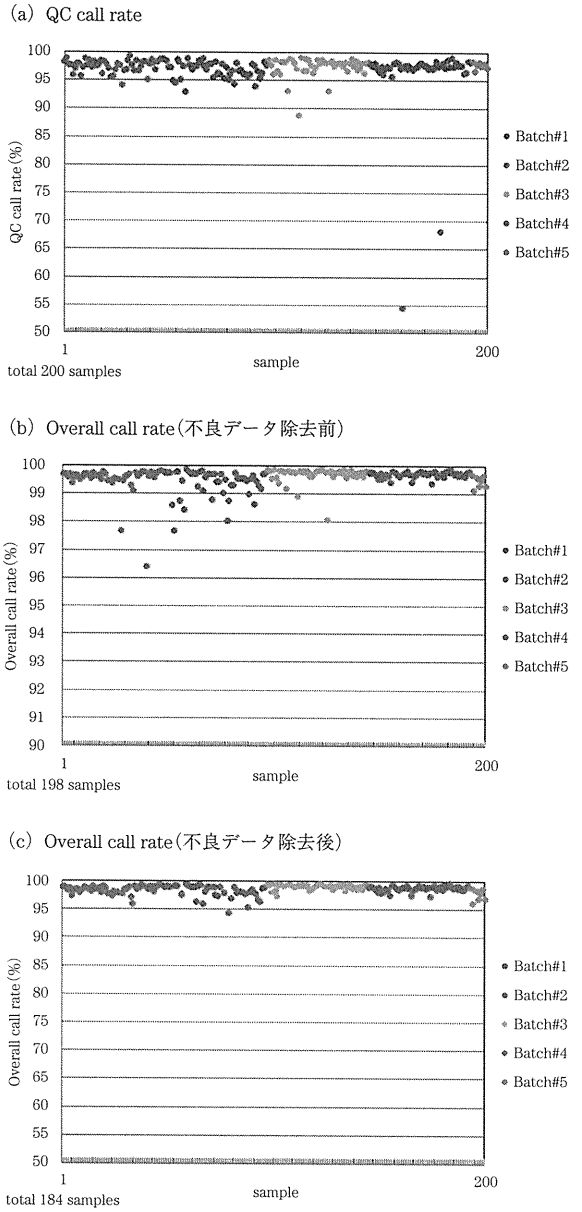

図2　SNP Array 6.0による日本人健常者200名のタイピング結果(口絵—4参照)

(a)クオリティーコントロール(QC)としてタイピングされた3,022 SNPsのコール率を示す。(b)QC call rateが86%を上回った198検体を用いて決定された全909,622 SNPsのコール率を示す。(c)QC call rateを指標として不良データを除去した後の184検体を用いて遺伝子型を決定した際の全909,622 SNPsのコール率を示す。

QC call rate が 86% を下回る検体は 200 検体のうち 2 検体であった(**図 2(a)**)。続いて，QC call rate が 86% を上回った 198 検体を用いて Overall call rate を決定したところ，平均 99.58% となった(**図 2(b)**)。

5. Birdseed アルゴリズムによる正確な遺伝子型決定方法

膨大な SNP データを取り扱うゲノムワイド関連分析において，タイピングエラーが原因で生じる偽陽性関連は解析を進めるうえで大きな障害となる。そこで，SNP Array 6.0 に搭載された全 90 万種の SNP について，できるだけ多くの SNP の遺伝子型を正確に決定する必要がある。遺伝子型決定に用いる Birdseed アルゴリズムの特性を知るために，日本人健常者 198 検体の中からランダムに 12 検体を選択し，その 12 検体を含む六つの異なるサンプルサイズ(12，24，36，48，72，96 検体)で決定した遺伝子型を，198 検体で決定した際の遺伝子型と比較した[18]。その結果，12 検体だけで遺伝子型を決定した際の Overall call rate は平均 99.84%(99.62～99.92)となり，検体数が増えていくと Overall call rate は下がり，198 検体で決定した際には平均 99.71%(98.07～99.89)となった(**図 3**)。一方，12 検体だけで決定した遺伝子型と 198 検体で決定した遺伝子型を比較した際の一致率(concordance)は，平均 99.47%(98.37～99.67)と最も低く，サンプルサイズが大きくなるにつれて一致率は上昇し，96 検体で遺伝子型を決定した際の一致率は平均 99.87%(99.40～99.92)となった(図 3)。この結果から，Birdseed アルゴリズムはサンプルサイズが小さくても遺伝子型を決定できるものの，高いタイピング精度を得るためには多くのサンプルを用いて遺伝子型を決定する必要があることが分かった。

Birdseed アルゴリズムによる遺伝子型決定において，サンプルサイズが大きくなるにつれて Overall call rate が低くなるという現象の原因として，QC call rate≥86% という閾値では十分に不良データを取り除けていないということが考えられる。日本人健常者 200 検体のタイピング結果から QC call rate と Overall call rate との間には強い相関があることが分かったため，QC call rate の閾値をより厳しくして不良データの除去を行った。QC call rate の閾値を 95% とすると 188 検体が閾値を上回り，Overall call rate は平均 99.65%(95.66～99.92)となった。しかし，厳しい閾値をパスした検体の中に，Overall call rate がより悪くなるものが見られた。それらをさらに除外し，最終的にすべての検体で Overall call rate が上昇するまで不良データの除去を繰り返したところ，184 検体が残り，Overall call rate は平均 99.71%(98.87～99.92)となった(**図 2(c)**)。

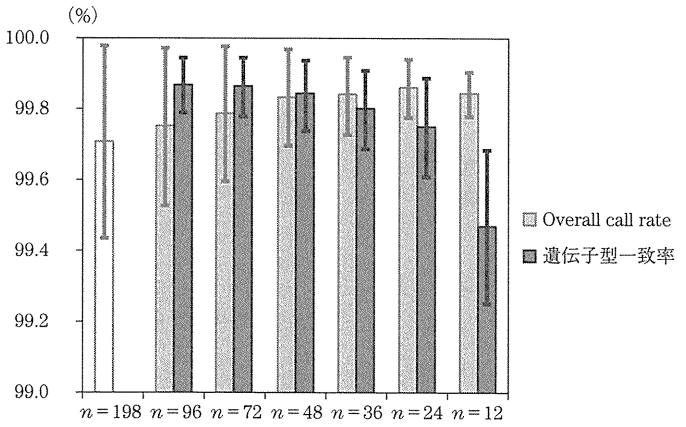

図 3　Birdseed アルゴリズムによる遺伝子型決定の精度
日本人健常者 198 検体の中からランダムに 12 検体を選択し，その 12 検体を含む六つの異なるサンプルサイズ(12，24，36，48，72，96 検体)で決定した遺伝子型を，198 検体で決定した際の遺伝子型と比較した。各サンプルサイズで遺伝子型を決定した際のその 12 検体の Overall call rate および遺伝子型一致率(concordance)を示す。

6. 日本人を対象としたSNP Array 6.0によるGWASの有用性

日本人健常者184検体のSNPタイピングの結果から，SNP Array 6.0に搭載された全909,622種のSNPのうち，約20%に相当する180,859 SNPsにおいて多型性が見られないことが明らかとなった。また，遺伝子型が決定されたSNPの中にはタイピング精度の悪いSNPが一部含まれており，それらのSNPは偽陽性関連の原因の一つになると考えられる。これについては，マイナーアリル頻度(MAF)，ハーディー・ワインバーグ平衡(Hardy–Weinberg equilibrium；HWE)およびSNP call rate(各SNPについて，タイピングした全検体のうち遺伝子型を決定できた検体の割合)を指標として，タイピング精度の悪いSNPの大部分を排除することができる[20]。筆者らの解析では，MAF>5%，HWE p値>0.001，SNP call rate>95%を満たすSNPは，590,248 SNPsとなり，また，MAF>1%，HWE p値>0.001，SNP call rate>95%を満たすSNPは661,559 SNPsとなった。この約59万種のSNPによりヒトゲノムの約75%をカバーできることから，日本人においてもSNP Array 6.0を用いたゲノムワイド関連解析が有用であることが期待される。

7. SNPタイピングデータのデポジット

文部科学省の「統合データベースプロジェクト」において，筆者らはSNPタイピングデータの半永続的な集約管理と研究者間の情報共有を目指して，日本人健常者のデータを登録した標準SNPデータベース，日本人健常者のコピー数多型(CNV)を登録したCNVデータベース，およびゲノムワイド関連解析のデータベース(GWAS–DB)を構築している[21]。GWAS–DBは，研究概要，品質基準などの情報とともに，遺伝子型頻度やアリル頻度，及び遺伝統計解析の結果を登録している。また，GWAS–DBはSNPだけでなくマイクロサテライトやCNVの疾患関連解析の結果も登録・閲覧することができ，エクソン情報やCNVなどの情報と遺伝統計解析の結果を重ね合わせて可視化する機能を備えている。疾患関連SNPの候補を多面的に選択できるよう，複数の機関が産出した同一疾患のデータ，および，異なるプラットフォームの解析結果を比較したり，メタ解析を行ったりする機能を搭載し，専門家以外にも利用しやすいデータベースの構築を目指している。

本研究でタイピングした日本人健常者200検体のSNP情報は，標準SNPデータベースに登録され，遺伝子型頻度やアリル頻度といった頻度情報は公開されている。また，今回タイピングした日本人健常者200検体のデータは，さまざまな多因子疾患を対象としたGWASにおいて共通のコントロール集団として用いられることが期待される。加えて，筆者らの研究室で行ったナルコレプシーを対象としたGWASの結果もGWAS–DBに登録され，遺伝統計解析の結果が公開されている。

8. 疾患感受性遺伝子の特定を目的とした新規SNPタイピング技術：DigiTag2法

筆者らはゲノムワイド連鎖分析あるいはゲノムワイド関連分析によって検出された候補領域において，第一義的な疾患感受性遺伝子多型を特定するため(絞り込み)に適する技術としてDigiTag2法を確立した[22][23]。DigiTag2法は，SNPの遺伝子型をDCN(DNA Coded Number)と呼ぶオリゴDNAへ変換してマルチプレックスSNPタイピングを行う(**図4**)。DCN(図4中，EDおよびD1)は物理的，化学的に性質が一様となるように設計した23塩基長のオリゴDNAで，DCNを使用することにより正確なDNA分子反応を行うことが可能となる。また，DCNは解析対象となるSNPに対して自由に割り当てることができるため，結果表示に用いるDNAチップは解析対象に依存せず汎用的に使用できるという特徴を持っている。また，解析対象となるSNP数にかかわらずラベリング反応に用いる蛍光プライマーが2種類で済むことから低コストでSNPタイピングを行うことが可能となる。

DigiTag2法は32種もしくは96種のSNPを1セットとして同時並列的にSNPタイピングを行う。これまでにいくつかの多因子疾患を対象とした絞り込み解析をDigiTag2法で行い，解析対象としたSNPの約9割でタイピング結果を得ることができ，また，平均99.48%という高いコール率でSNPタ

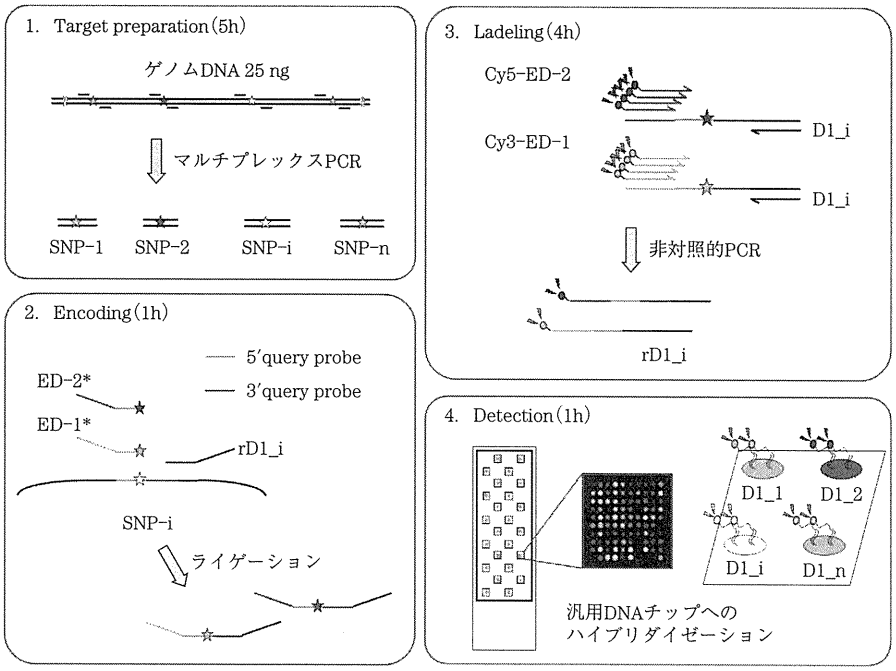

図4　DigiTag 2法の概要(口絵—5参照)

DigiTag 2法は，ターゲット分子調製，エンコード，ラベリング，検出の四つの工程で構成される。5′query probeにはアリルに対応して2種類のED(ED-1，ED-2)を付加し，また3′query probeにはSNPに応じてD1(D1_i)を付加する。EDおよびD1は物理的，化学的性質が一様となるように設計した23塩基長のオリゴDNAである。配列が相補鎖である場合には配列名称の前に"c"を付けた。

イピングを行えることが明らかとなった。DigiTag 2法は高い成功率でSNPタイピングを行えることから，ゲノムワイド連鎖分析あるいはゲノムワイド関連分析によって検出された候補領域における絞り込み解析を効率的に行う技術として確立することが期待される。

9. おわりに

90万種以上のSNPを一挙にタイピングできる技術の実用化によって，従来は存在しなかった広範かつ詳細なヒトゲノム多型情報が得られる時代となった。しかしながら同時に，われわれはまだ得られる膨大な多型情報を十分に活用できるノウハウを持っていないことも指摘しておきたい。筆者らの用意した統計解析ソフトウェアは個々のSNPについては関連分析を行えるものの，ハプロタイプについての関連分析はできない。市販のソフトウェアにも，限定した領域でハプロタイプ関連分析できるものはあるものの，ゲノム全域にわたって一挙に分析できるものはない。また，タイピングした検体の中には血縁関係にあるものや検体の重複などが含まれている可能性がある。血縁者が含まれていることが擬陽性の増幅につながることが知られており，それらの関連分析に不適切な検体を取り除くことも真の疾患関連遺伝子を検出するためには重要となる。さらに，多数の検体について得られたゲノムワイド多型解析情報から，これまで全く知られていなかった新しい遺伝子／遺伝子相互作用が見いだされる可能性がある。しかし残念ながら，従来の統計学的手法や計算アルゴリズムでは，このように膨大なデータを実用的に処理できない。このように，ゲノムワイド多型解析情報はバイオインフォマティクスに関わるさまざまな研究者にとって挑戦に値する多くの課題を提供してくれるとともに，その達成によって従来にない実り豊かな成果をもたらしてくれるに違いない。

【引用・参考文献】

1) J. Ohashi and K. Tokunaga : *J. Hum. Genet.*, **46**, 478–482(2001).